

Buckling Instability of Self-Assembled Colloidal Columns

James W. Swan,^{*} Paula A. Vasquez,[†] and Eric M. Furst[‡]

Department of Chemical and Biomolecular Engineering, Center for Molecular and Engineering Thermodynamics, University of Delaware, Newark, Delaware 19716, USA

(Received 28 February 2014; revised manuscript received 7 August 2014; published 23 September 2014)

Suspended, slender self-assembled domains of magnetically responsive colloids are observed to buckle in microgravity. Upon cessation of the magnetic field that drives their assembly, these columns expand axially and buckle laterally. This phenomenon resembles the buckling of long beams due to thermal expansion; however, linear stability analysis predicts that the colloidal columns are inherently susceptible to buckling because they are freely suspended in a Newtonian fluid. The dominant buckling wavelength increases linearly with column thickness and is quantitatively described using an elasto-hydrodynamic model and the suspension thermodynamic equation of state.

DOI: 10.1103/PhysRevLett.113.138301

PACS numbers: 82.70.Dd, 83.80.Hj, 87.80.Ek, 87.80.Nj

The scientific study of buckling and its application to engineering problems begins with Leonhard Euler [1] and has informed thought on subjects as varied in scale as the maximum height of trees [2], the compressive strength of living cells [3], and the mechanical failure of carbon nanotubes [4]. The buckling of thin films on mismatched substrates is a significant challenge in modern engineering of hard materials [5], ranging from semiconductors to thermal barrier materials [6]. There is now also the potential to exploit buckling and other elastic instabilities in the design and engineering of new soft material structures, including polymer interfaces [7], elastomers and gels [8], thin liquid films [9], and active biopolymer networks [10]. Despite these emerging applications, anticipating the non-linear and often complex behavior of such instabilities remains a significant challenge.

In this Letter, we report experiments performed in microgravity that reveal a unique buckling instability in slender, self-assembled domains of magnetically responsive colloidal particles. Upon cessation of the magnetic field that drives their assembly, columns of paramagnetic colloids expand axially and buckle laterally. This phenomenon most closely resembles the buckling of long beams due to thermal expansion as can happen to continuously welded railway tracks [11]. However, in the present experiment, we show that the stability of these slender domains has a different character from expanding rails on an elastic foundation. The colloidal columns are *inherently* susceptible to buckling because they are freely suspended in water. Their buckling is distinct in a class of elasto-hydrodynamic instabilities in soft materials, which includes the coil-stretch transition of macromolecules [12,13] and the buckling of elastic filaments [14,15] in flow.

In the microgravity environment aboard the International Space Station (ISS), aqueous suspensions of paramagnetic latex colloids with radius $a = 525$ nm (Dynabead MyOne, Invitrogen) and zeta potential $\zeta \approx -45$ mV are suspended

in ultrapure water (< 1% by volume). We estimate the Debye length to be on the order of $\kappa^{-1} \approx 300$ nm. The relatively high specific density of these magnetic beads $\rho \approx 1.4$ leads to strong sedimentation in a gravitational field. The gravitational length $l_g = 3kT/4\pi g\Delta\rho a^3$ is approximately 1 μm , where $\Delta\rho$ is the difference between the particle and medium densities and g is the acceleration due to gravity. The particles are assembled through the application of a uniform magnetic field generated by a Helmholtz coil. Such particles initially form chains aligned with the magnetic field lines [16]. These chains interact attractively and rapidly form a sample-spanning network of particles that is kinetically arrested. We have shown that toggling the magnetic field off and then on again with a prescribed frequency and sufficient length of time anneals this system-spanning structure, causing it to condense into locally ordered domains aligned with the magnetic field and having a high aspect ratio [17]. The formation of these colloidal columns occurs at toggle frequencies between 0.66 and 20 Hz at a 50% duty cycle. The columnar domains are shown in Fig. 1, along with an illustration of their location in the sample. The samples are held in glass capillaries that are 2 mm wide parallel to magnetic field, 0.2 mm deep, and approximately 50 mm long. The capillaries are supported rigid in custom fabricated aluminum sample holders that insert into the Helmholtz coil assembly. The optical assembly consists of two digital video (DV) cameras (Hitachi HV-C20, 768×494 pixels, 30 fps) and a fiber bundle light source. Columns are imaged in the center of the capillary with a long working distance objective. The distances between the columns and the capillary walls are sufficient to minimize hydrodynamic interactions. Movies of the experiments were recorded on DV tape and returned to Earth for image processing and analysis.

Slender domains or columns of the assembled paramagnetic colloids buckle each time the magnetic field that

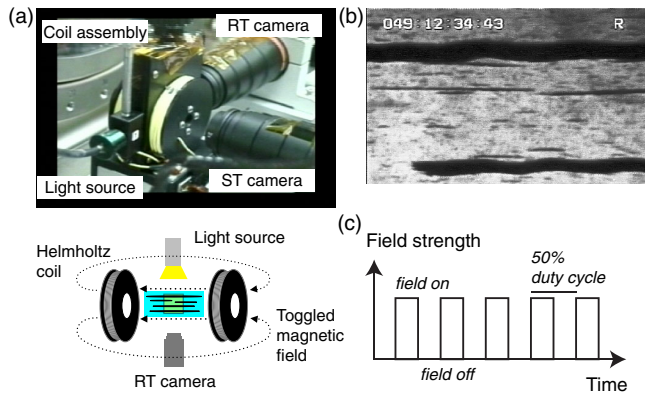


FIG. 1 (color online). (a) The position of the columns in the field is illustrated in the experimental apparatus as installed in the microgravity sciences glovebox onboard the ISS. (b) The RT camera with field of view transverse to the magnetic field images columnar structures that form after toggling the field. The dark regions are the condensed colloidal columns. (c) The field is toggled with a 50% duty cycle for more than one hour at frequencies between 0.66 and 20 Hz.

drives them to assemble is switched off, as shown in Fig. 2. A movie of the buckling is provided as Supplemental Material [18]. One view is that the magnetic field acts to confine the particles locally. The loss of free volume and their ordering reduces the entropy of the suspension. When the field is on, that reduction in entropy is balanced by the magnetic interaction energy. However, when the field is off, the particles must reequilibrate. The reduced entropy now acts like a normal stress that drives the columns to expand. An equivalent view is that the magnetic field serves as a thermostat for an attractive particle phase. High magnetic field strengths are equivalent to a reduction in the effective temperature, quenching the suspension into a condensed state. Thus when the magnetic field is turned off, the effective temperature increases and the self-assembled columns undergo thermal expansion. For either view, in the moment when the field is turned off, the columns behave as prestressed beams. The fluid in which they are suspended resists their expansion, and a buckling instability results.

We measured the wavelength associated with this buckling as a function of the column width in 12 separate experiments conducted aboard the ISS (Fig. 2). The conditions of the experiments were varied in magnetic field strength (1–2.2 kA/m), toggle frequency (0.66–2 Hz) and particle volume fraction (0.04%–0.065%). As illustrated in Fig. 3, there is an obvious linear trend in the buckling wavelength as a function of column width, W . (Fig. 2). When multiple periods were observed for a single column, each wavelength was included in our analysis, which accounts for the scatter in the data. For domains thinner than $30 \mu\text{m}$ in width, the wavelength grows as $(4.6 \pm 0.1)W$, with the coefficient determined by a linear least squares fit. For domains thicker than $30 \mu\text{m}$, the

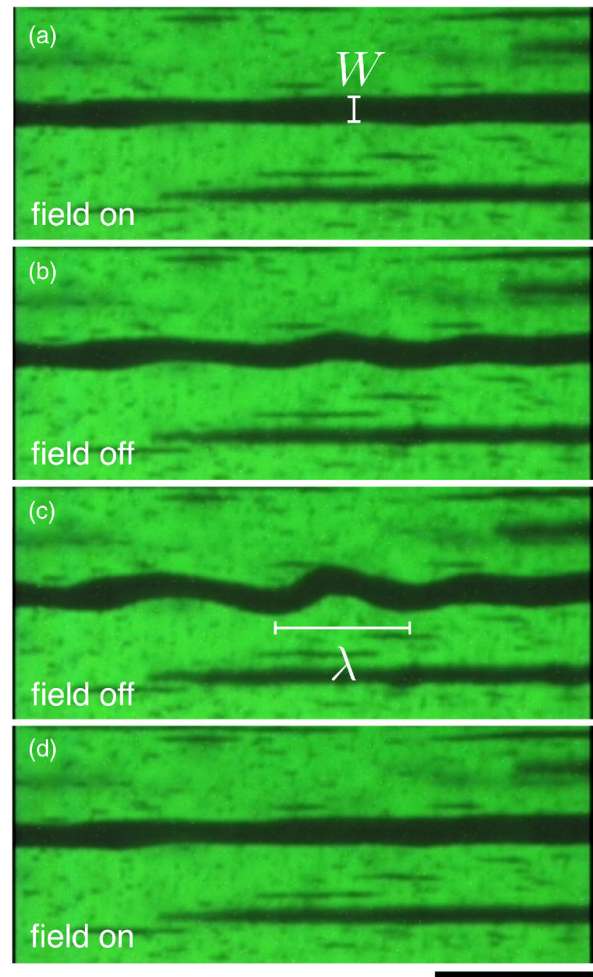


FIG. 2 (color online). A column in its (a) unbuckled, field-on state. (b) Subsequent growth of the buckling instability when the field is toggled off. (c) The maximum deflection. (d) The column returning to the unbuckled state as the field toggles on. The magnetic field is oriented left to right. The field strength is 2 kA/m and the toggle frequency is 0.66 Hz. The scale bar is $100 \mu\text{m}$.

wavelength of the buckling instability falls below this linear trend. From video micrographs of the samples, we observe that the aspect ratio of the domains is larger than 100 to 1. The thickest domains span the entire sample in the field direction (width, 2 mm), and therefore are not freely suspended. Such wide columns also exert strong magnetic forces on one another with an interaction energy that scales linearly with the column volume. In this circumstance the columns are reinforced, which has been shown to reduce the buckling wavelength of suspended beams and microtubules [19]. The linear trend for thinner, freely suspended columns can be explained by elastohydrodynamic theory.

The mechanics of elastic filaments in a viscous medium have been investigated in detail previously [14,15,20,21]. Similarly, we consider a slender elastic column of length L and width W with $W/L \ll 1$, immersed in a viscous fluid and subject to a uniform axial stress, $P > 0$. The lateral

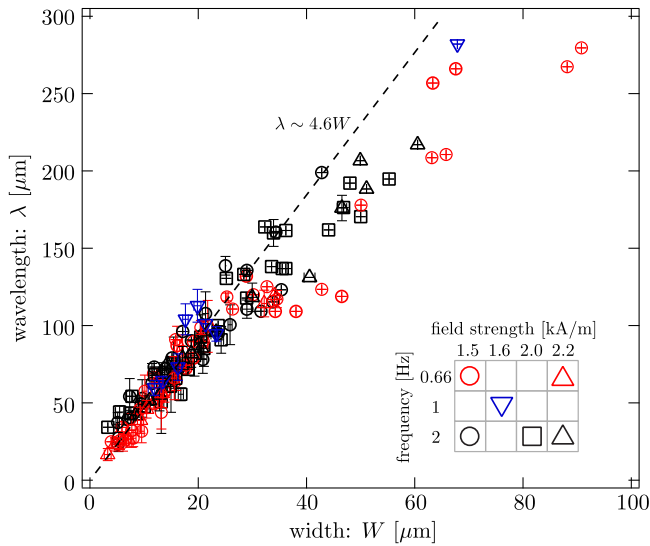


FIG. 3 (color online). The buckling wavelength versus domain width measured in 12 separate experiments with domains assembled with different magnetic field strengths and pulse frequencies.

displacement of this column, $y(x, t)$, as a function of the position along its axis, x and time, t , can be represented as the elastica [22]

$$-EIy_{xxxx} - PAy_{xx} - \xi_{\perp}y_t = 0. \quad (1)$$

The first term is the lateral force that acts to resist bending. The elastic modulus of the column is denoted E while I is its area moment of inertia—assumed constant and proportional to W^4 . The second term represents the lateral force on a bent column produced by the imposed axial stress, where A is the column cross-sectional area and proportional to W^2 . The third term is the lateral force exerted by the fluid due motion of the column. The quantity, ξ_{\perp} , is the hydrodynamic resistance per unit length of the column subject to motions perpendicular to its axis. From slender body theory, applicable in the limit $W/L \ll 1$, this hydrodynamic resistance is known to be well approximated by the value [21,23] $4\pi\eta/[\ln(2L/W) + 1/2]$, where η is the fluid viscosity. Thus it has only a weak, logarithmic, dependence on the column geometry.

The stability of the column is assessed by proposing a small lateral deformation with wavelength λ that grows in time with rate ω [6,19]: $y(x, t) \sim \exp(2\pi ix/\lambda + \omega t)$. The parameters of such a perturbation are determined by substitution into Eq. (1), which yields the dispersion relation:

$$EI\left(\frac{2\pi}{\lambda}\right)^4 - PA\left(\frac{2\pi}{\lambda}\right)^2 + \xi_{\perp}\omega = 0. \quad (2)$$

The fastest growing perturbation will satisfy the conditions: $d\omega/d\lambda = 0$ and $\omega > 0$. The first condition specifies the wavelength of this perturbation,

$$\lambda = 2\pi\sqrt{2EI/(PA)}. \quad (3)$$

Solving the dispersion relation for the growth rate associated with this wavelength, we find that

$$\xi_{\perp}\omega = (PA)^2/(4EI), \quad (4)$$

which is indeed positive and independent of the column width.

Next, we solve for the elastic modulus in terms of the growth rate and replace the cross-sectional area with $\pi W^2/4$. The fastest growing wavelength can be written as explicitly linear in the width of the domain:

$$\lambda = \pi\sqrt{\frac{\pi P}{2\xi_{\perp}\omega}}W. \quad (5)$$

The linear relationship between λ and W is a common feature of an elastic buckling instability, and could be anticipated from other buckling phenomena, such as the buckling wavelength of thin films on viscous substrates [6], elastic rods subject to compression [24], or microtubules dispersed in an elastic gel [19]. The linear scaling relation of Eq. (5) agrees with the experimental observations in Fig. 3. The coefficient of proportionality is composed of quantities that may be estimated in the following way.

First, we consider the colloids making up the column as effective hard spheres. These particles must diffuse collectively in order for the column to move at all. Therefore, the maximum growth rate ω is limited by the thermal relaxation rate of the particles based on their diffusivity $\omega = D/a^2$, where a is the particle radius. Then, $D/a^2 = CkT/\eta a^3$, where C is a dimensionless constant to be determined. On substitution of this rate, we find the proportionality constant

$$\lambda \approx W\sqrt{\frac{3\pi\phi}{32C}\left(\ln\left[\frac{2L}{W}\right] + \frac{1}{2}\right)\left(\frac{P}{nkT}\right)}, \quad (6)$$

with n denoting the particle number density within the column and $\phi = 4\pi na^3/3$ denoting the particle volume fraction based on the hydrodynamic radius. Next, the quantity P/nkT is the compressibility factor which may be determined from an equation of state [25]. The magnetic interactions are roughly 100 times stronger than thermal stresses. Therefore, we estimate the effective hard-sphere volume fraction in the columns approaches 68%—that for a maximally packed body-centered-cubic crystal. At this concentration, the compressibility factor for hard spheres is $P/nkT \approx 37$. Finally, note that the aspect ratio L/W is intrinsic and must be the same for any widely separated and well equilibrated columns. From micrographs of the columns, this ratio appears to be larger than 100 to 1. This estimate for the coefficient of proportionality is insensitive to modest variation in both the compressibility

and the aspect ratio since it depends on the square root of the former and the logarithm of the latter.

After making the substitutions above, $\lambda \approx 6.6C^{-1/2}W$, leaving only the constant C , the magnitude of the relaxation, to be determined. One estimate is to assume that the structure relaxes with a rate given by the particle self-diffusivity, $D_0 = kT/6\pi a\eta$. In this case, $C = 1/6\pi \approx 0.05$ and $\lambda \approx 29W$, which is much greater than the experimental proportionality constant, 4.6. The relaxation rate $\omega = D_0/a^2$ is too slow; it would lead to buckling wavelengths that are significantly longer than those that are observed. The results instead suggest that the relaxation is governed by *collective* diffusion, for which $D = D_0K(\phi)$ ($d[\phi_{\text{eff}}Z(\phi_{\text{eff}})]/d\phi_{\text{eff}}$), where $K(\phi)$ is the sedimentation coefficient that accounts for the many-body hydrodynamic interactions between particles [26] and $Z(\phi_{\text{eff}}) = P/nkT$. The sedimentation coefficient depends on the volume fraction of the hydrodynamic cores: ϕ , whereas the osmotic compressibility depends on an effective hard sphere volume fraction that includes the double layer repulsion between particles, $\phi_{\text{eff}} = \phi(1 + 1/\kappa a)^3$. This is the effective hard-sphere volume fraction in the solid column that determines its osmotic pressure ($\phi_{\text{eff}} \approx 0.68$), but electrostatic repulsion between spheres means the volume fraction of the solids is smaller. With the compressibility of the columns again given by the solid equation of state [25] and the sedimentation coefficient from well-known solutions of the Stokes equations [27], we find $C \approx 5$ and $\lambda \approx 3W$, in better agreement with the experiment. With reasonable approximations, the collective diffusion of the constituent particles accounts for the rate of expansion of the columns and resulting buckling wavelengths. Interestingly, because both the diffusivity and hydrodynamic drag depend on the fluid viscosity, the buckling wavelength predicted by Eq. (6) is expected to be independent of this property.

The instability expressed by Eq. (4) predicts that, unlike the buckling of a prestressed beam on an elastic support such as a railway track [28], there is no critical stress below which buckling of suspended colloidal columns is suppressed. A prestressed column in a viscous fluid is inherently unstable. Our observations agree, at least in part, with the theory. Figure 4 shows the buckling state diagram that summarizes the field strengths and frequencies for which buckling is observed in the microgravity experiments. The closed symbols indicate the occurrence of buckling, while open symbols represent an absence of measurable buckling. Naturally, buckling is not observed above a critical frequency that corresponds to a ramified network suspension structure, which scales as $\nu \sim H^{-4/3}$ [17]. Above this frequency, the suspension does not relax to freely suspended columns. Below the critical frequency, however, both buckling and nonbuckling conditions are observed.

For freely suspended columns, buckling requires both a large enough prestress generated by the induced magnetic interactions, which scales as $\sim H^2$, and a toggle frequency

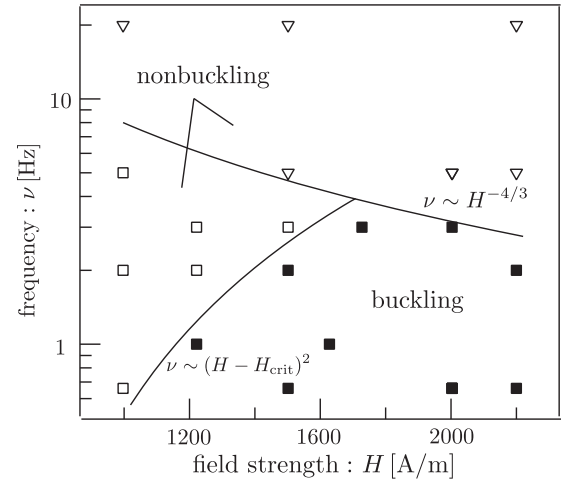


FIG. 4. Buckling occurs for field strengths and frequencies indicated by closed symbols, but is not observed at high frequencies when the suspension structure is sample spanning (open triangles) or at low field strengths for free, suspended columns (open squares).

that provides sufficient time for the instability to grow to a perceptible amplitude. This transition is captured by the functional form $\nu \sim (H - H_{\text{crit}})^2$ with $H_{\text{crit}} \approx 600$ A/m, and is also shown in Fig. 4. We hypothesize that H_{crit} is related to a melting transition of the solidlike columns to a more fluidlike state, and thus a lower osmotic pressure driving the expansion. Additionally, at lower field strengths, growing defects in the solid column structure, such as grain boundaries, could accommodate the strain when the field is toggled off, thus limiting their tendency to buckle.

These experiments have demonstrated and quantified the way in which condensed domains of paramagnetic colloids disassemble upon cessation of the magnetic field driving their assembly. These domains behave like a prestressed beam freely suspended in a Newtonian fluid. The forces that drive the particles to disperse when the magnetic field is toggled off also generate a stress in the self-assembled domains that cause them to buckle. This simple but unique microgravity experiment adds to what is known of buckling phenomena. Furthermore, while the field-directed self-assembly of micrometer and nanometer sized particles into condensed, ordered phases allows for rapid and high fidelity formation of microstructured materials with useful optical, electrical, mechanical, and thermal properties [29–31], these experiments provide insight into how such highly structured materials *disassemble*.

The authors thank astronauts Peggy A. Whitson, E. Michael Fincke, Koichi Wakata, Sandra H. Magnus, Frank De Winne, and Michael R. Barratt for their assistance in performing experiments aboard the ISS, members of the scientific support team at NASA Glenn Research Center and ZIN Technologies, and Marc Fermigier, Olivia du Roure, and Julien Heuvings for fruitful discussions.

Support from NASA (Grants No. NAG3-1887, No. NAG3-2398, No. NAG3-2832, No. NNX07AD02G and No. NNX10AE44G) is gratefully acknowledged. E. M. F. thanks the ESPCI Chaire Joliot program.

*Present address: Department of Chemical Engineering, Massachusetts Institute of Technology, 77 Massachusetts Ave., Cambridge, MA 02139.

†Present address: Department of Mathematics, University of South Carolina, 313D LeConte College, 1523 Green Street, Columbia, SC 29208.

‡furst@udel.edu

- [1] L. Euler, *Opera Omnia* 1 **24**, 231 (1744).
- [2] A. G. Greenhill, *Proc. Cambridge Philos. Soc.* **4**, 65 (1881).
- [3] M. E. Chicurel, C. S. Chen, and D. E. Ingber, *Curr. Opin. Cell Biol.* **10**, 232 (1998).
- [4] M. R. Falvo, G. J. Clary, R. M. Taylor, V. Chi, F. P. Brooks, S. Washburn, and R. Superfine, *Nature (London)* **389**, 582 (1997).
- [5] M. Grinfeld, *Europhys. Lett.* **22**, 723 (1993).
- [6] N. Sridhar, D. J. Srolovitz, and Z. Suo, *Appl. Phys. Lett.* **78**, 2482 (2001).
- [7] J. Kim, J. A. Hanna, M. Byun, C. D. Santangelo, and R. C. Hayward, *Science* **335**, 1201 (2012).
- [8] S. Cai, K. Bertoldi, H. Wang, and Z. Suo, *Soft Matter* **6**, 5770 (2010).
- [9] L. Espín, A. Corbett, and S. Kumar, *J. Non-Newtonian Fluid Mech.* **196**, 102 (2013).
- [10] T. Sanchez, D. Chen, S. J. DeCamp, M. Heymann, and Z. Dogic, *Nature (London)* **491**, 431 (2012).
- [11] D. F. Cannon, K. O. Edel, S. L. Grassie, and K. Sawley, *Fatigue Fract. Eng. Mater. Struct.* **26**, 865 (2003).
- [12] P.-G. de Gennes, *J. Chem. Phys.* **60**, 5030 (1974).
- [13] C. M. Schroeder, H. P. Babcock, E. S. G. Shaqfeh, and S. Chu, *Science* **301**, 1515 (2003).
- [14] L. E. Becker and M. J. Shelley, *Phys. Rev. Lett.* **87**, 198301 (2001).
- [15] L. Guglielmini, A. Kushwaha, E. S. G. Shaqfeh, and H. A. Stone, *Phys. Fluids* **24**, 123601 (2012).
- [16] A. P. Gast and C. F. Zukoski, *Adv. Colloid Interface Sci.* **30**, 153 (1989).
- [17] J. W. Swan *et al.*, *Proc. Natl. Acad. Sci. U.S.A.* **109**, 16023 (2012).
- [18] See Supplemental Material at <http://link.aps.org/supplemental/10.1103/PhysRevLett.113.138301> for columns of paramagnetic colloids buckling in a toggled field. The magnetic field is oriented left to right. The field strength is 2 kA/m and the toggle frequency is 0.66 Hz. The frame is 360 μm wide.
- [19] C. P. Brangwynne, F. C. MacKintosh, S. Kumar, N. A. Geisse, J. Talbot, L. Mahadevan, K. Parker, D. Ingber, and D. A. Weitz, *J. Cell Biol.* **173**, 733 (2006).
- [20] C. H. Wiggins and R. E. Goldstein, *Phys. Rev. Lett.* **80**, 3879 (1998).
- [21] M. J. Shelley and T. Ueda, *Physica (Amsterdam)* **146D**, 221 (2000).
- [22] L. D. Landau, L. P. Pitaevskii, E. M. Lifshitz, and A. M. Kosevich, *Theory of Elasticity*, 3rd ed. (Elsevier Butterworth-Heinemann, Oxford, 1986).
- [23] J. B. Keller and S. I. Rubinow, *J. Fluid Mech.* **75**, 705 (1976).
- [24] J. R. Gladden, N. Z. Handzy, A. Belmonte, and E. Villermaux, *Phys. Rev. Lett.* **94**, 035503 (2005).
- [25] K. R. Hall, *J. Chem. Phys.* **57**, 2252 (1972).
- [26] G. K. Batchelor, *J. Fluid Mech.* **52**, 245 (1972).
- [27] A. S. Sangani and A. Acrivos, *Int. J. Multiphase Flow* **8**, 343 (1982).
- [28] S. P. Timoshenko and J. M. Gere, *Theory of Elastic Stability*, 2nd ed. (Dover Publications, Mineola, 1989).
- [29] M. Grzelczak, J. Vermant, E. M. Furst, and L. M. Liz-Marzan, *ACS Nano* **4**, 3591 (2010).
- [30] B. Dong, T. Zhou, H. Zhang, and C. Y. Li, *ACS Nano* **7**, 5192 (2013).
- [31] P. Reineck, G. P. Lee, D. Brick, M. Karg, P. Mulvaney, and U. Bach, *Adv. Mater.* **24**, 4750 (2012).